End-Hall Processing with a Nonplanetary Rotating Stage
Staff of Kaufman & Robinson, Inc.

INTRODUCTION

End-Hall ion sources[1,2] are used for cleaning, ion-assisted deposition, and etching.[3,4]   The work pieces in these applications are usually mounted on rotating stages. Process uniformity is seldom a problem when the rotation is planetary, due to the forgiving nature of this motion.

Process uniformity requires more care with nonplanetary rotating stages. The ion beam is often directed toward the center of the stage in an attempt to utilize as much of it as possible. This results in a low ion-current density near the edge of the stage and a poor overall uniformity. Good uniformity is obtained with a nonplanetary rotating stage by directing the ion beam closer to the edge of the stage than its center. Directing the ion beam in this manner reduces the fraction of the ion beam intercepted by the stage, but this reduction is necessary to obtain good uniformity.

CALCULATION MODEL

The nonplanetary configuration that is analyzed is shown in Fig. 1. The end-Hall ion source assumed in this analysis is cylindrical, although linear versions are also available. The stage radius is R_{stg}, while the center of the exit plane of the ion source is displaced from the axis of stage rotation by the radius R_{src}. The axis of the ion source is at an angle α to the axis of rotation. The stage is assumed to be planar for this analysis, although other shapes are possible (e.g., see dashed lines in Fig. 1).

The beam shape from a cylindrical end-Hall ion source is approximated with an angular distribution of

$$j = j_o cos^n \Theta, \qquad (1)$$

where n is the beam-shape parameter, jo is the ion current density on axis at a given distance from the ion source, and j is the ion current density at the same distance but at an angle Θ from the axis [5]. The profile given by Eq. (1) would be directly applicable to an ion beam directed at a spherical surface with the center of the ion-source exit plane located at the center of the sphere (see Fig. 2).

If the ion current density is measured on a flat plane oriented normal to the axis of the ion beam (again see Fig. 2), the relationship is

$$j = j_o cos^{n+3} \Theta. \qquad (2)$$
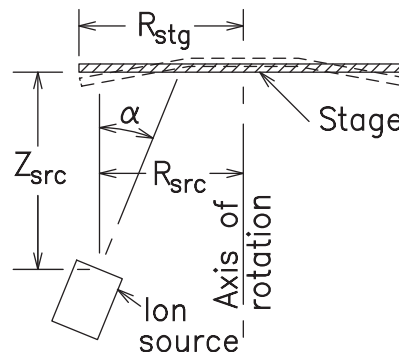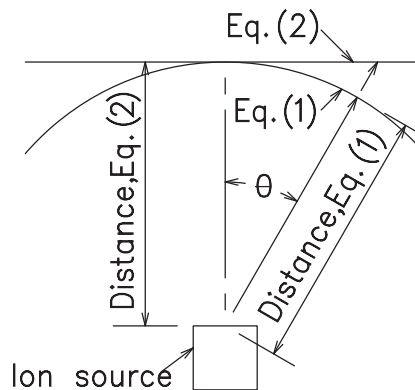

Fig. 1. Nonplanetary configuration.

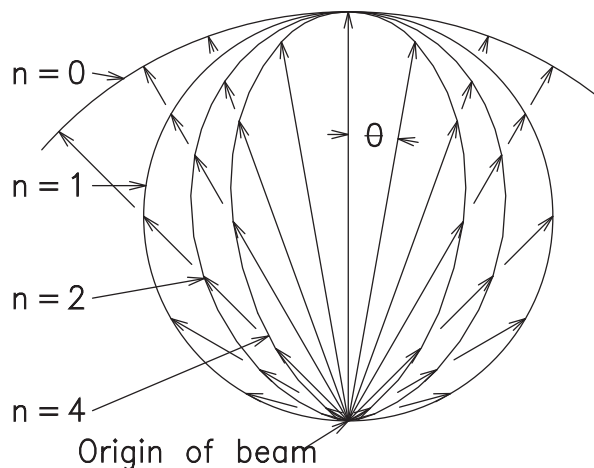**Fig. 2. Survey locations for the ion current densities, j, given by Eqs. (1) and (2).**

Fig. 3. Angular distributions for Eq. (1). The length of an arrow indicates the current density at that angle.
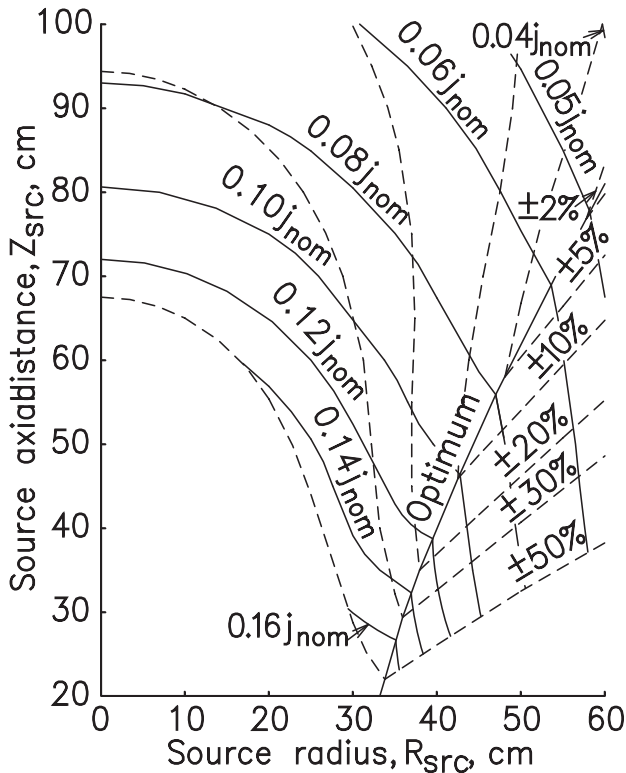
Fig. 4. Mean current density and uniformity for α = 0, a beam-shape parameter, n, of 2 and a planar, rotating nonplanetary stage with a radius of 50 cm.

Fig. 5. Minimum current density and uniformity for α = 0, a beam-shape parameter, n, of 2 and a planar, rotating nonplanetary stage with a radius of 50 cm.

The experimental ion-beam profiles supplied by ion source manufacturers have been measured both at spherical locations, Eq. (1), and planar locations, Eq. (2). The beam-shape parameters, n, of these profiles vary from less than 1 to nearly 4, as shown in Fig. 3 for Eq. 1.

CALCULATION PROCEDURE
A numerical calculation was carried out at stage radii from 0 to 100% of the maximum radius, in 5% steps of that maximum radius. At each radius, the current densities were averaged over 72 equally-spaced circumferential locations. (The averaging is done by stage rotation in the actual application.) The mean ion current density for each combination of source radius, R_{src}, and source distance, Z_{src}, is the average of the maximum and minimum values obtained over the entire range of radius. This mean ion current density is expressed as a fraction of the nominal ion current density, j_{nom}, which is defined as the ion current density measured on the beam axis at distance of 30 cm from the exit plane of the ion source. At
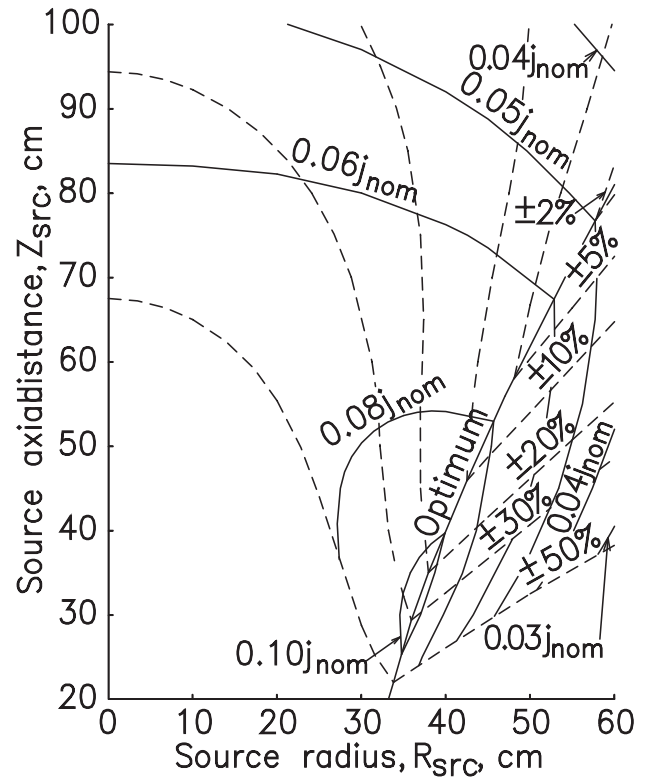
a given angle from the beam axis, Θ, the ion current density varies inversely as the square of the distance from an axial location in the exit plane. This inverse-square relationship is quite accurate for distances greater than about 15-20 cm from the ion source. The uniformity for each combination of source radius, R_{src}, and source distance, Z_{src} is half of the difference of the maximum and minimum values obtained over the entire radius range, divided by the mean ion current density. Other parameters could have been used, such as a weighted mean or a statistical distribution about the mean value. However, the parameters used herein are easy to define and are often used in thin-film applications.

CALCULATED RESULTS
Mean current density and uniformity are shown in Fig. 4 for a an ion-source angle, α, of zero and a range of both source radius, R_{src}, and source distance, Z_{src}. The beam-shape parameter, n, equals 2 for Fig. 4, and the stage radius, R_{stg}, is 50 cm. There is a locus of source locations shown by the line labeled optimum, which, for each source distance Z_{src}, gives
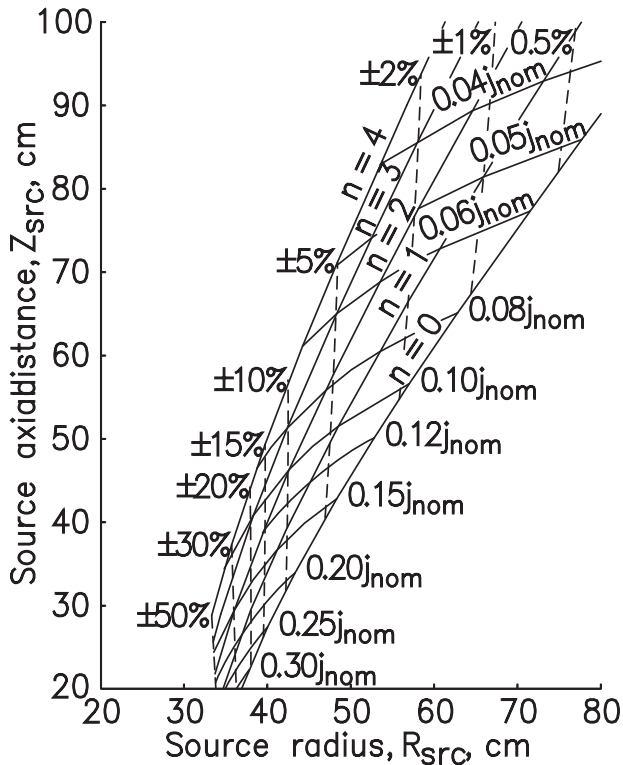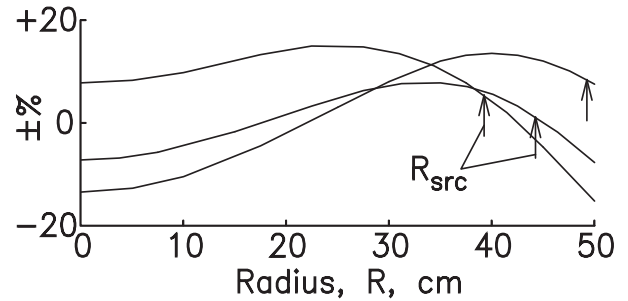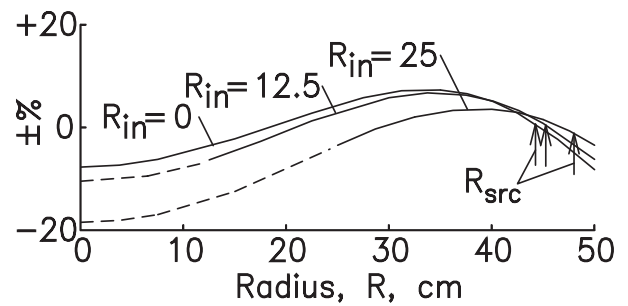
Fig. 6. Mean current density and uniformity for α=0, a planar, rotating nonplanetary stage with a radius of 50 cm. Source radius is optimized for beam-shape parameters from 0 to 4.

(a) Effect of source radius.

(b) Effect of stage inside radius.

Fig. 7. Radial variation in current density and uniformity for α=0, a beam-shape parameter, *n*, of 2 and a planar, rotating nonplanetary stage with a radius of 50 cm. The source distance, Z_{src}, is also 50 cm.

the most uniform current density over the stage. It will be shown that the optimum ion-source angle, α, is not far from zero for a given source distance, Z_{src}. Also, the beam-shape parameter, n, of 2 is typical in that it is an intermediate value. The qualitative trends shown in Fig. 4 should therefore be fairly general.

Both the ion current density and uniformity degrade as the source radius, R_{src}, increases above the optimum value. But it appears from Fig. 4, that, for a given axial spacing, Z_{src}, a reduction in radius, R_{src}, from the optimum value of this parameter might provide a useful tradeoff between ion current density and uniformity. This possibility is examined in Fig. 5 by plotting the same results shown in Fig. 4, but using *minimum* ion current densities instead of *mean*. In Fig. 5, decreasing the source radius below the optimum value at a given axial spacing results in a much smaller increase in ion current density - it actually decreases at axial spacings, Z_{src}, less than about 50 cm.

Comparing Figs. 4 and 5, it is apparent that the increase in *mean* current density as R_{src} is reduced from the optimum value is accompanied by little or no improvement in *minimum* ion current density. In general, if a minimum current density is to be maintained, there is little or no net advantage for operating at a radius, R_{src}, less than the optimum value for any given axial spacing, Z_{src}.

The mean current density and uniformity are shown in Fig. 6 for the optimum source radius, R_{src}, at each source distance, Z_{src}. The stage radius, R_{src}, is again 50 cm. The beam-shape parameter, *n*, covers the range of 0 through 4. Although Fig. 6 is limited to an ion-source angle, α, of zero, it is a compact presentation of many of the important results of this investigation.

The calculated results presented in Figs. 4 and 6 show the mean ion current density and the maximum variation from that mean. More detailed radial variations of ion current density are shown in Fig. 7. The effect of source radius on

that variation is shown is shown in Fig. 7(a). The middle source radius (44.3 cm) is the optimum radius, giving a maximum variation of ±7.7% from the mean value. At this condition, the current density near the outer edge of the stage equals the current density near the axis of rotation. The two other source locations are ±5 cm from the optimum radius. In experimentally selecting an optimum source radius, processing results, such as ion-assist properties or etch depth, should be made equal near the axis of rotation and near the outer edge of the stage.

The effect on the current-density distribution of optimizing for an annular area instead of the entire stage area is shown in Fig. 7(b), with R_{in} the inside radius of the annular region. The portions of the current-density distributions at radii less than R_{in} are shown in Fig. 7(b) as dashed lines. Because of the slow variation in current density with radius near the axis of rotation, increasing R_{in} from zero to 12.5 cm (25% of the outside radius of 50 cm) results in the optimum radius of the ion source increasing from 44.3 cm to only 45.3 cm. The further increase of R_{in} to 25 cm has a much larger effect, however, increasing the optimum source radius to 48.1 cm. In general, moderate unused areas near the axis of rotation will have little effect on the optimum source radius.

The analysis up to this point has been limited to a source angle, α, equal to zero and, except for Fig. 6, a beam-shape parameter, *n*, of 2. Figures 8 through 11 show the effect of varying the source angle, α, on current densities and uniformities for beam shape parameters of one through four. The values shown in these figures are solutions for which the combinations of angle, α, and radius, R_{src}, have been optimized for uniformity. For example, the angle, α, can be considered optimized for each combination of distance, Z_{src}, parameter, *n*, and radius, R_{src}. Or conversely, the radius, R_{src}, can be considered optimized for each combination of distance, Z_{src}, parameter, *n*, and angle, α. Note that the equivalent of these figures is available for *n* equal to zero from Fig. 6, because α has no effect for this value of *n* - at least for the range of angle from the source axis, Θ, used to evaluate the parameter, *n*.

Examination of Figs. 8 through 11 will show that, for a given value of source axial distance, the maximum mean current density is found at a source angle, α, of zero to ten degrees. This is the basis of the earlier statement that the optimum ion-source angle, α, is not far from zero for a given source distance, Z_{src}. It may appear that a larger value of ion-source angle may be useful to improve the uniformity, but the use of larger angles would also require larger values of source radius, R_{src}, which are often not possible due to the close proximity of

the vacuum-chamber walls. Although the information in Figs. 8 through 11 is not as compact as that in Fig. 6, it can be used to evaluate options in which the source angle, α, is not equal to zero.

SCALING
A single stage radius of 50 cm was used for the calculated results presented in Figs. 4 through 11 to facilitate comparisons of the results in different figures. The conversion of results shown in these figures to other stage sizes is fairly simple. A conversion can be made between stage sizes 1 and 2 if:

$$(R_{src}/R_{stg})_1 = (R_{src}/R_{stg})_2, \tag{3}$$

$$(Z_{src}/R_{stg})_1 = (Z_{src}/R_{stg})_2, \tag{4}$$

$$n_1 = n_2. \tag{5}$$

If the conditions of Eqs. (3) through (5) are satisfied, then the uniformity will be the same for the two stage sizes and the mean current density will be given by

$$(j_{mean}R_{stg}^2)_1 = (j_{mean}R_{stg}^2)_2. \tag{6}$$

Note that Eq. (6) is equivalent to conservation of ion-beam current. That is, the product of the stage area and the mean ion current density must be the same for the two stage sizes.

As a more specific example, if all the dimensions (Rstg, Rsrc, and Zsrc) are doubled and the beam-shape parameter is the same, then the mean current density from the same ion source will be reduced by a factor of four.

EXPERIMENTAL CONSIDERATIONS

Ion Dose
The ion dose is the mean ion-current density times the duration of ion-source operation, and has the units of mA-sec/cm². The required ion dose for cleaning and ion-assist applications can be estimated using a publication by Kaufman and Harper.[3,6] The required dose for etching can be estimated from sputter yields and, if available, the variation of sputter yields with angle of incidence.
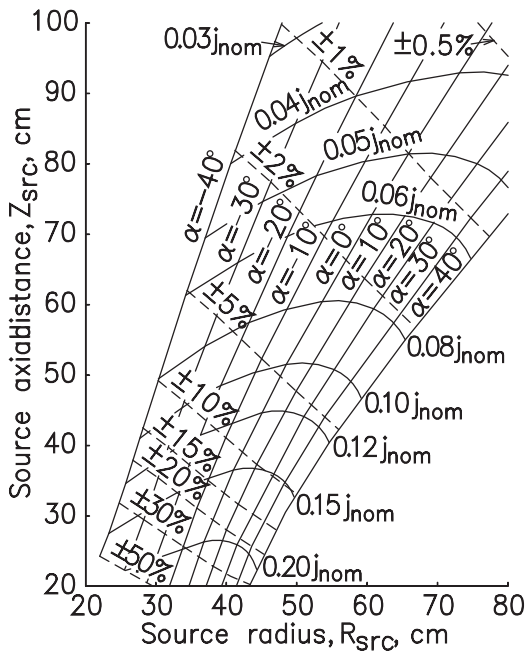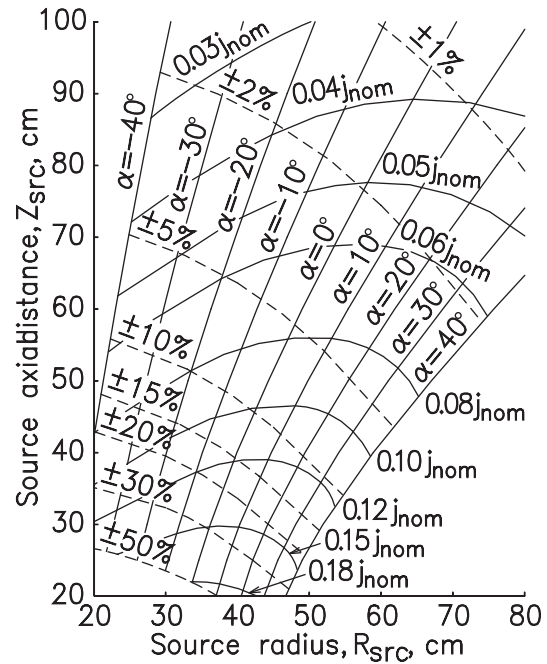
Fig. 8. Mean current density and uniformity for *n*=1.
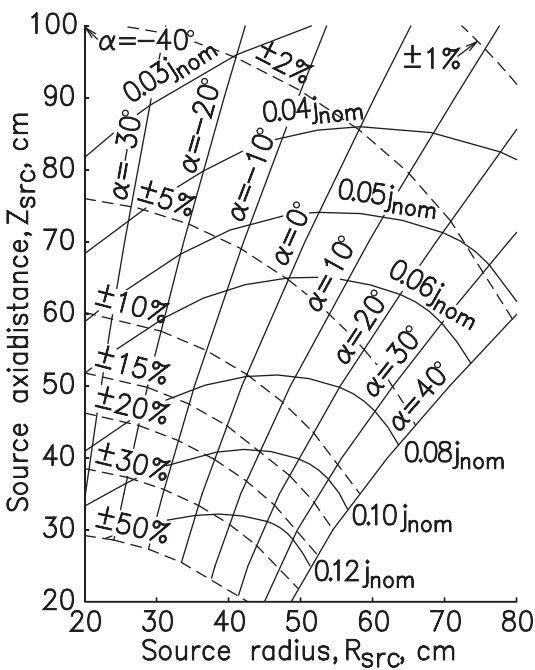

Fig. 9. Mean current density and uniformity for *n*=2.

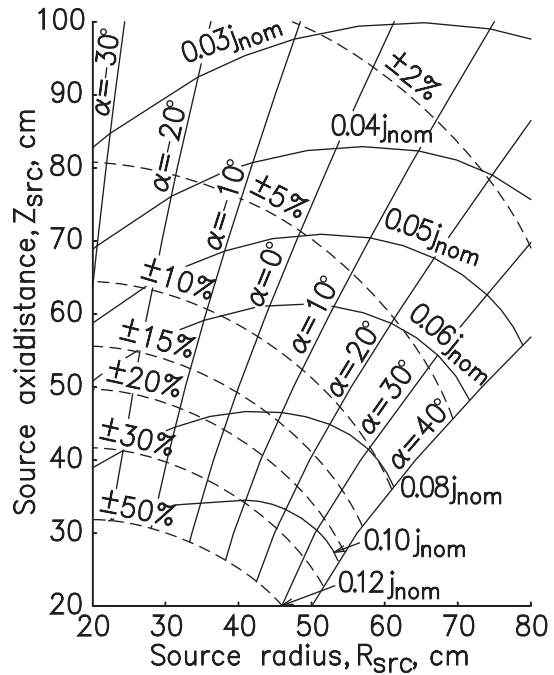**Fig. 10. Mean current density and uniformity for *n*=3.**

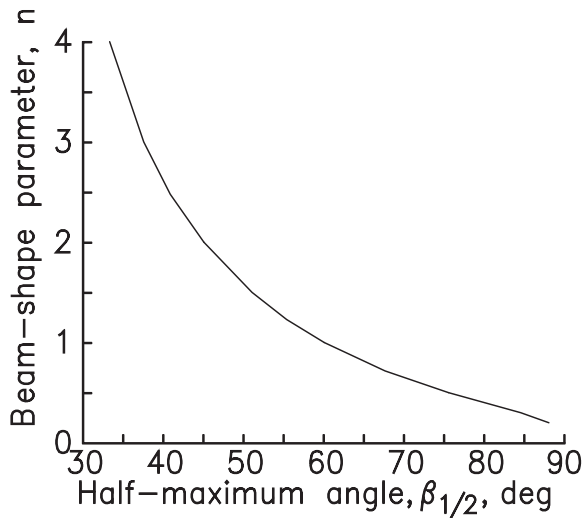**Fig. 11. Mean current density and uniformity for *n*=4.**

Fig. 12. Relationship between half-maximum angle and beam-shape parameter at a constant distance (Eq. (1)).
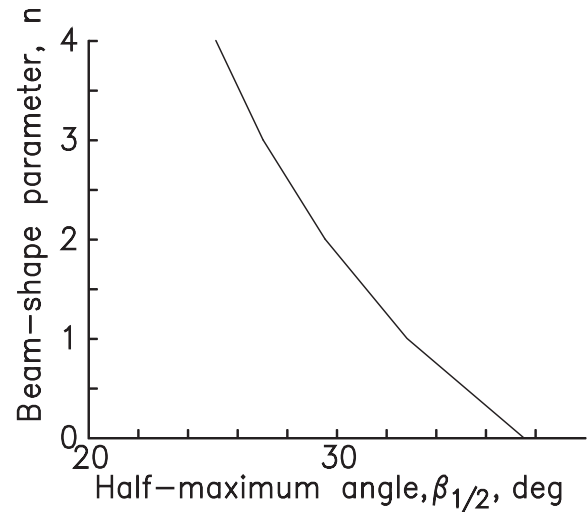

Fig. 13. Relationship between half-maximum angle and beam-shape parameter at a flat plane (Eq. (2)).

Source Location

If the stage radius of interest is other than 50 cm, the scaling relationships, Eqs. (3) through (6), should be used to convert the values of ion current densities, Z_{src}, and R_{src} presented herein to the values for that stage radius.

To select a configuration that gives good uniformity with a particular ion source, it is necessary to obtain the beam-shape parameter, n. The first step is to obtain the ion-beam profile for your ion source for an operating condition close to the one you want to use. That profile should be available from the manufacturer of the source. From the ion-beam profile, find the angle from the source axis where the current density is half the on-axis value, which herein is called the half-maximum angle, $\beta_{1/2}$. Use that angle to find the beam-shape parameter with either Fig. 12 or Fig. 13, depending on how the beam profile was obtained. Figure 12 is for a profile obtained at a constant distance from the ion source (Eq. (1)), while Fig. 13 is for a profile obtained at flat plane normal to the axis of the ion beam (Eq. (2)).

Using the value of n obtained as described above, different combinations of R_{src} and Z_{src} can be obtained from Fig. 6. Each combination of R_{src} and Z_{src} will have a corresponding mean ion-current density and uniformity. The best combination of mean current density and uniformity should be selected for the application of interest. This will often be the highest mean current density that will give acceptable uniformity.

The optimum values of R_{src} and Z_{src} obtained in the manner described above are the solution for an ion-source angle, α, of zero. If these values can be used without interference from other hardware installed in the vacuum chamber, they should be tried. If the experimental results are satisfactory, they can be used for the permanent location of the ion source.

If the experimental results are *not* satisfactory, it is often because the uniformity is poor. Using Fig. 7(a) as a guide, the source should be moved to a larger value of R_{src} if there is an indication of low current density near the outer edge of the stage, or moved to smaller value of R_{src} if there is an indication of low current density over a fairly broad region near the axis of rotation.

Figures 8 through 11 can be used for other combinations of R_{src} and Z_{src}, and their corresponding values of mean current density and uniformity, for values of α not equal to zero. The advantages in mean current density and uniformity from Figs. 8 through 11 over the values from Fig. 6 ($\alpha = 0$) will generally be small, but it may be important to move the ion source to avoid interference with other vacuum-chamber hardware. It can also be more convenient for final adjustments in uniformity to change the ion-source angle instead of changing the ion-source radius.

A planar stage was used in the calculation model. Other shapes are possible, as indicated by the dashed lines in Fig. 1. It is not practical to cover all possible stage shapes in this paper. Instead, it is suggested that an initial solution be found by assuming a planar stage, then experimentally iterate to optimize uniformity for the actual stage shape. It should be apparent that the initial solution will be most accurate for stages that approximate a planar shape.

Etching applications can present special problems due to the effect of angle of incidence on sputter yield. Depending on the material being etched, the shape of the etch profile at a planar stage can be approximately the same as that of the ion-beam profile, or it can be flatter.[4] If the etch profile is available, more accurate results can be obtained by determining the beam-shape parameter from the etch profile. This approach, however, is best used for an ion-source angle, α, of zero. (The etch profile would effectively be displaced from the ion-beam profile at a planar stage with an ion-source angle other than zero.) The mean etch rate can be obtained by multiplying the fraction of j_{nom} (from Fig. 6, for example) by the on-axis etch rate at 30 cm.

In the absence an etch profile or detailed knowledge of angle-of-incidence effects, the ion-beam profile should be used to determine the beam-shape parameter, and the calculated on-axis etch rate at 30 cm should be used with j_{nom} to determine the mean etch rate, again with α = 0. Such an approach will usually give conservative etch rates and uniformities, as well as slightly low values of R_{src}.

Wall Effects
The broad ion beam from an end-Hall ion source is useful for the uniform coverage of a stage. But the broad ion beam can also cause problems when part of it strikes the vacuum-chamber wall, causing material to be sputtered from the wall onto the stage. A detailed treatment of this problem is not practical here, but a few comments will indicate the nature of the solutions.

If the process of interest is etching, it may be difficult to increase the etching rate near the outer edge of the stage to equal the rate near the axis of rotation. This can be due to sputtering from the vacuum-chamber wall increasing as the source radius R_{src} is increased. Thus, although the etch rate near the outer edge is increased as R_{src} is increased, what is observed is the smaller net etch rate that includes removing the deposition from the wall. Good etch uniformity can still be obtained by using baffles to intercept the ions that would strike the vacuum-chamber wall, with the sputtered surfaces

of the baffles oriented so that they do not "see" the stage. In general, baffles can be designed by assuming that ions and sputtered particles both follow straight-line trajectories, as long as any baffle is not close enough to interfere with ion-source operation (about 15-20 cm). Possible baffle locations are shown in Fig. 1 of Ref. 6. Experimental measurements of the effects of baffles are described in Ref. 4.

As an alternative solution, the ion beam can be directed more toward the axis of rotation of the stage, making the wall impingement negligible; but masks must then be used to intercept part of the ion beam and reduce the etch rate of the rest of the stage to equal the etch rate near the edge. The design of such masks is more complicated than the design of the baffles described above.

Similar problems can occur with contamination of a deposited film, with deficiencies in the absorption, color, or stability of the film deposited near the edge of the stage. If such problems are found, the vacuum-chamber wall near the ion source should be examined. If the wall appears to be significantly cleaner near the source, the cleaned area is a likely source of contamination. The same solutions can be used as were given above for etching: use baffles to prevent sputtered material from the wall from reaching the stage, or move the source toward the axis of rotation and mask the rest of the ion beam to reduce the current density there to the value near the edge.

Speed of Rotation
The location of the ion source at one side of the stage results in a circumferential variation of the ion current density. The number of rotations during a process should be large enough that the particular location of a work piece relative to the ion source at the start of the process should have a small effect on the ion dose received. This number of rotations divided by the operating time for the ion source gives a minimum speed of rotation.
There is another limitation on the speed of rotation for ion-assist applications. Deposition is usually fairly uniform over the stage area. The circumferential nonuniformity of the ion-current density thus results in alternate excesses of deposition and ion arrivals as the stage rotates. Even at energies less than 100 eV, the ions have the capability to compact or otherwise modify the deposited film to a depth of several atomic layers. In general, the speed of rotation described in the preceding paragraph will be high enough that circumferential variations in ion-current density will occur too rapidly to have adverse effects.

REFERENCES

1. H.R. Kaufman, R. S. Robinson, and R. I. Seddon, "End-Hall Ion Source," *J. of Vacuum Science and Technology A*, Vol. A5, pp. 2081-2084, July/Aug. 1987.

2. H.R. Kaufman and R. S. Robinson, "End-Hall Ion Source," *U.S. Patent* 4,862,032, Aug. 29, 1989.

3. H.R. Kaufman, J.M. E. Harper, "Ion-Assist Applications of Broad-Beam Ion Sources," *Proceedings of SPIE*, 5527, pp. 50-68. Aug. 2004.

4. J.R. Kahn and H.R. Kaufman, "Low-Energy Ion-Beam Etching," *Proceedings of SVC 49th Annual Technical Conference,* Washington, DC, Apr. 2006.

5. H.R. Kaufman and R.S. Robinson, *Operation of Broad-Beam Sources*, Commonwealth Scientific Corporation, Alexandria, Virginia, 1987, pp. 65-66.

6. Anon., "Ion-Assist Doses," *Technical Note* KRI-05, Kaufman & Robinson, Inc., 2006.